Chapter 1

Introduction

As one of the most important materials in the Nano area, carbon nanotubes have generated broad and interdisciplinary attention in the last two decades. Carbon Nanotube (CNTs) was discovered by Sumio Iijima[1] in 1991. After the discovery, CNTs have found enormous importance for many applications in the field of nanotechnology, electronics, sensors and optics, due to their unique electrical and mechanical properties, and extremely high aspect ratio. Over the last couple of decades potential efforts have been dedicated to predict and measure the electrical properties (resistance, inductance and capacitance) of CNTs [2-4]. After the first report of FET fabrication using SWCNT (single walled carbon nanotube) [5], it has widely been used to fabricate Diode, MOSFET, and Bipolar devices. Large scale integration using CNTs has been reported by Rao *et al* [6]. CNTs have been introduced as a new material for potential applications in inter-chip and intra-chip interconnections [7], antenna material for GHz to THz technology [8-10]. With the predicted progress towards nanometer-scale feature sizes, GHz clock rates, and microwave wireless communications, there is a growing need to understand the properties of circuits, interconnects, devices, and antennas with Nano-scale dimensions. Carbon nanotubes offer a combination of small size, high mobility, large current density (about 10^9 A/cm) [11] and low intrinsic capacitance; moreover, their intrinsic cut-off frequency is expected to be high. Therefore they are among the candidates to eventually candidate for GHz to THz Nano-antennas.

Creating a compact, reliable source of terahertz (THz) radiation is one of the most challenging problems in contemporary applied physics [12]. Even though THz technology is at the boundaries of microwave and photonic technologies; it is quite underdeveloped compared to the achievements in the microwave or the photonic technology. There are very few commercially available instruments for the THz frequency region, and most of them lack the precision required to perform accurate measurements. There are also no miniaturized and low-cost THz sources.

One of the latest trends in THz technology [13] is to use single-walled carbon nanotubes (SWNTs) as building blocks of novel high-frequency devices.

CNTs have different structure and properties. According to that, CNTs can be both SWCNT or Multi walled Carbon Nanotube (MWCNTs). Even though Double Walled Carbon Nanotube (DWCNT) is a kind of MWCNT but still it is called differently as DWCNT as it showed some unique properties as it is the transition model between SWCNTs and MWCNTs. SWCNTs are of various kinds such as zigzag, chiral, and armchair. These are formed upon different formation of the graphene. Zigzag CNTs work as insulator as these have high resistivity whereas chiral CNTs work as semiconductor and armchair CNTs work as conductor.

In this work our aim is to study the electromagnetic wave propagation characteristics of SWCNT. For that purpose, we shall predict the attenuation constant and phase constant of EM wave while propagating through SWCNT and investigate the effects of frequency and diameter of SWCNT on those parameters.

References

[1] I. Iijima, "Helical microtubules of graphitic carbon," *Nature*, vol. 354, pp. 56–58, (1991)

[2] R. Saito, G. Dresselhaus, and M. S. Dresselhaus, "*Physical Properties of Carbon Nanotubes,"* London, U.K.: Imperial College Press, (2003).

[3] P.J Burke, "Luttinger liquid theory as a model of the Gigahertz electrical properties of carbon nanotubes," IEEE Trans.On Nanotechnol. Vol. 1, No.3, (2002)

[4] P. J. Burke, "An RF Circuit Model for Carbon Nanotubes," *IEEE TRANSACTIONS ON NANOTECHNOLOGY,* vol. 2, NO. 1, MARCH 2003.

[5] S. J Tans, A. R. M Verschueren and C. Dekker, "Room-temperature transistor based on a single carbon nanotube," *Nature*, vol 393, p. 49, (1998).

[6] S. G. Rao, L. Huang, W. Setyawan, S. Hong, "Large-scale assembly of carbon nanotubes," *Nature*, vol. 425, p36, (2003).

[7] Y. Y. Sun, L. Zhu, H. Jiang, J. Lu, W. Wang and C.P. Wong, "A Paradigm of Carbon Nanotube Interconnects in Microelectronic Packaging," *J. Electronic materials*, vol. 37, pp1691-1697 (2008).

[8] G. W. Hanson,"Fundamental Transmitting Properties Properties of Carbon Nanotube Antennas," *IEEE Trans. on Antenna and Propag*, Vol. 53, pp.3426-3435, (2005).

[9] Jin Hao and G.W Hanson, "Infrared and Optical Properties of Carbon Nanotube Dipole Antennas, " *IEEE Trans. Nanotechnol*. Vol.5, pp. 766-775, (2006).

[10] Yi Huang, Wen-Yan Yin, *Senior Member, IEEE*, and Qing Huo Liu, "Performance Prediction of Carbon Nanotube Bundle Dipole Antennas," *IEEE Trans. on Nanotechnol.*, Vol. 7, pp.331-337, (2008).

[11] P.L McEuen, M.S. Fuhrer, H.K Park, "Single-walled carbon nanotube electronics," *IEEE Trans. Nanotechnol*., vol. 1, pp.78-85 (2002).

[12] Mark Lee, Michael C. Wanke, "Searching for a Solid-State Terahertz Technology Science" 6 April 2007: Vol. 316 no. 5821 pp. 64-65 DOI: 10.1126/science.1141012

[13] D Dragoman, M Dragoman, Terahertz fields and applications, Progress in Quantum Electronics 28 (1), 1-66 2004a

Chapter 2

Properties of Carbon Nanotube

2.1 Types of CNTS

There are three types of carbon nanotubes: armchair, zig-zag and Chiral (helical) nanotubes. These differ in their symmetry. Namely, the carbon nanotubes can be thought of as graphene planes 'rolled up' in a cylinder (the closing ends of carbon nanotubes cannot be obtained in this way). Depending on how the graphene plane is 'cut' before rolled up, the three types of carbon nanotubes are obtained. These tubes can be extremely long (several hundreds of nanometers and more). When produced in materials, carbon nanotubes pack either in bundles (one next to another within a triangular lattice) - single-walled carbon nanotubes, or one of smaller radius inside others of larger multi-walled carbon nanotubes.

2.2.1 Single Walled Carbon Nanotubes

Most single-walled nanotubes (SWCNT) have a diameter of close to 1~2 nanometer, with a tube length that can be many millions of times longer. The structure of a SWCNT can be conceptualized by wrapping a one-atom-thick layer of graphite called graphene into a seamless cylinder. The way the graphene sheet is wrapped represented by a pair of indices (n, m). Integers n and m denote the number of unit vectors along two directions in the honeycomb crystal lattice of graphene. If $m = 0$, the nanotubes are called zigzag nanotubes, and if $n = m$, the nanotubes are called armchair nanotubes otherwise, they are called chiral (See fig 2.2).

The diameter of an ideal nanotube can be calculated from its (n, m) indices as follows:

$$d = \frac{a}{\pi}\sqrt{n^2 + nm + m^2}$$

Where; $a = 0.246$ nm.

SWCNTs are an important variety of carbon nanotube because most of their properties change significantly with the (n, m) values, and this dependence is non-monotonic [5]. In particular, their band gap can vary from zero to about 2 eV and their electrical conductivity can show metallic or semiconducting behavior. Single-walled nanotubes are likely candidates for miniaturizing electronics. The most basic building block of these systems is the electric wire, and SWCNTs with diameters of an order of a nanometer can be excellent conductors [6][7]. One useful application of SWCNTs is in the development of the first intermolecular field-effect transistors (FET). The first intermolecular logic gate using SWCNT FETs was made in 2001 [8].To create a logic gate you must have both a p-FET and an n-FET. Because SWCNTs are p-FETs when exposed to oxygen and n-FETs otherwise, it is possible to protect half of an SWCNT from oxygen exposure, while exposing the other half to oxygen. This results in a single SWCNT that acts as a NOT logic gate with both p and n-type FETs within the same molecule.

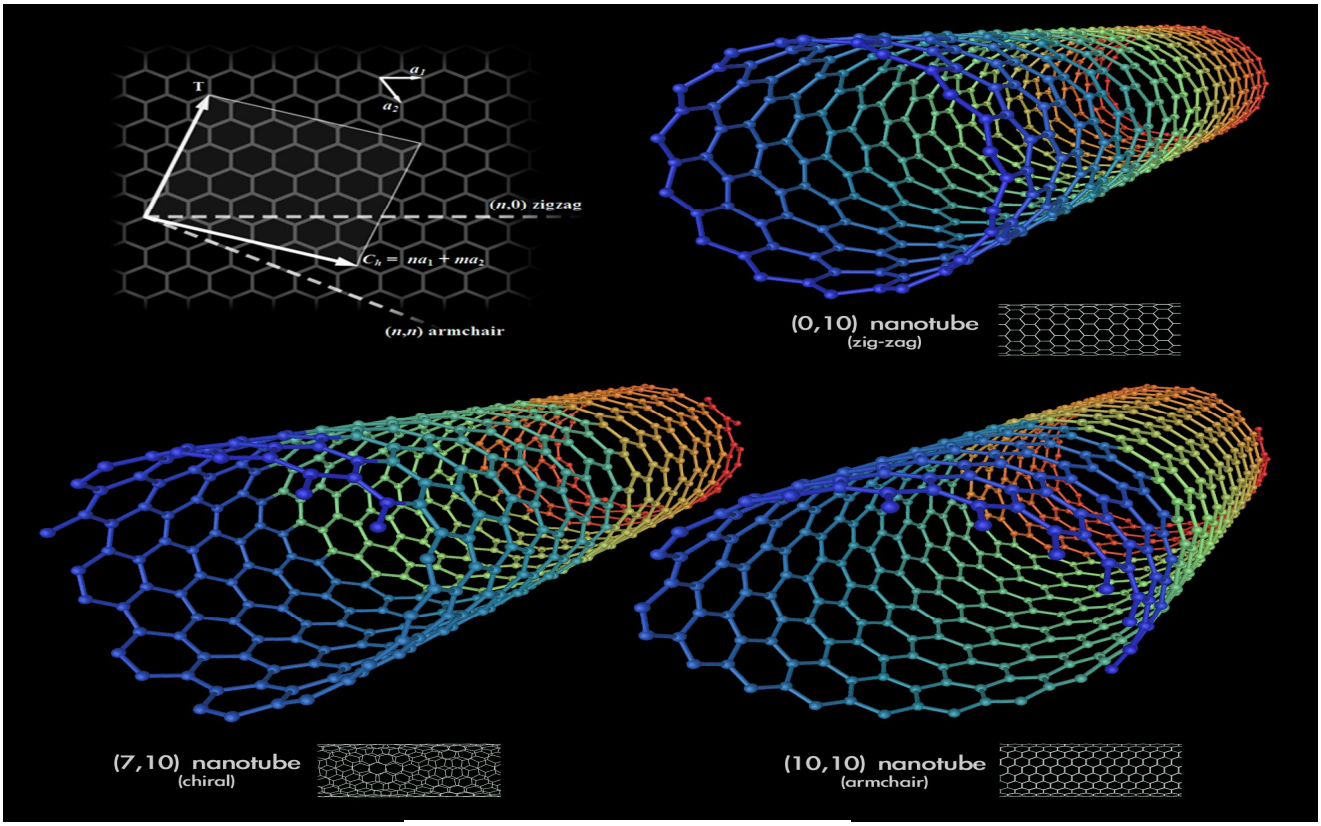

Fig 2.1 Different types of SWCNT

2.2.2 Multi Walled Carbon Nanotube

Multi-walled nanotubes (MWCNT) consist of multiple rolled layers (concentric tubes) of graphene. There are two models that can be used to describe the structures of multi-walled nanotubes. In the Russian Doll model, sheets of graphite are arranged in concentric cylinders, e.g., a (0, 8) SWCNT within a larger (0, 17) SWCNT. In the Parchment model, a single sheet of graphite is rolled in around itself, resembling a scroll of parchment or a rolled newspaper. The interlayer distance in multi-walled nanotubes is close to the distance between graphene layers in graphite, approximately 3.4 Å. The Russian Doll structure is observed more commonly. Its individual shells can be described as SWCNTs, which can be metallic or semiconducting. Because of statistical probability and restrictions on the relative diameters of the individual tubes, one of the shells, and thus the whole MWCNT, is usually a zero-gap metal.

Double-walled carbon nanotubes (DWCNT) form a special class of nanotubes because their morphology and properties are similar to those of SWCNT but their resistance to chemicals is significantly improved. This is especially important when functionalization is required (this means grafting of chemical functions at the surface of the nanotubes) to add new properties to the CNT. In the case of SWCNT, covalent functionalization will break some C=C double bonds, leaving "holes" in the structure on the nanotube and, thus, modifying both its mechanical and electrical properties. In the case of DWCNT, only the outer wall is modified. DWCNT synthesis on the gram-scale was first proposed in 2003[9] by the CCVD technique, from the selective reduction of oxide solutions in methane and hydrogen.

The telescopic motion ability of inner shells [10] and their unique mechanical properties [11] permit to use multi-walled nanotubes as main movable arms in coming Nano mechanical devices. Retraction force that occurs to telescopic motion caused by the Lennard-Jones interaction between shells and its value is about 1.5 nN [12].

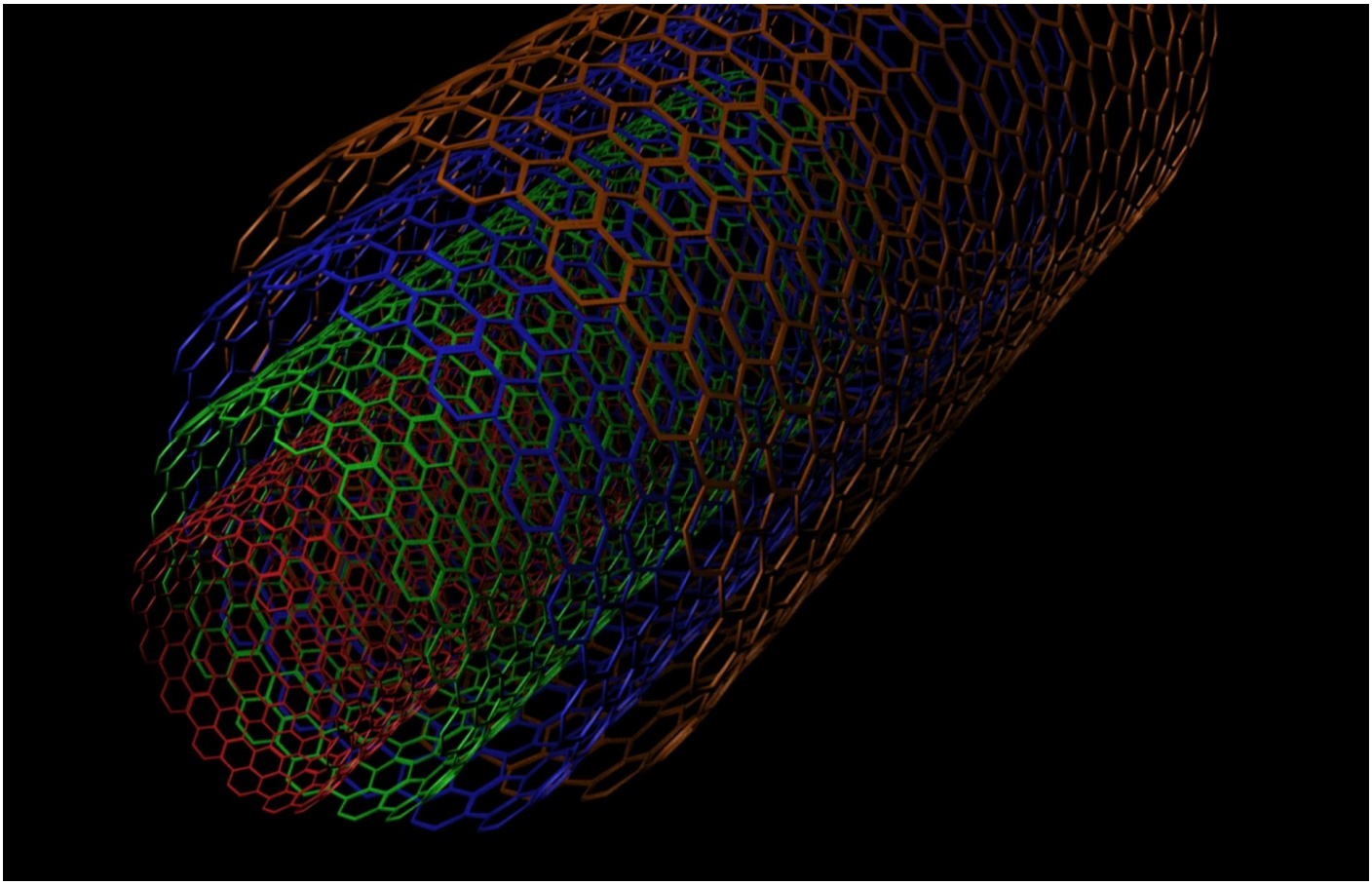

Fig 2.2 Structure of MWCNT

There are some other types of CNTs also such as Torus, Nano-bud, Graphenated carbon nanotubes (g-CNTs), Peapod, etc.

2.3 Properties of CNTs

Properties of CNTs are quite different than the material we generally use. These properties made CNTs such important material for using in Nano technology and also in high frequency region. Some properties are discussed below in general. Properties for high frequency antenna are discussed in detail in the later chapter.

2.3.1 Strength

CNTs are the strongest and stiffest materials yet discovered in terms of tensile strength and elastic modulus respectively. This strength results from the covalent sp2 bonds formed between the individual carbon atoms. In 2000, a multi-walled carbon nanotube was tested to have a tensile strength of 63 Giga Pascal (GPa) [13]. (For illustration, this translates into the ability to endure tension of a weight equivalent to 6422 kg on a cable with cross-section of 1 mm2.) Further studies, conducted in 2008, revealed that individual CNT shells have strengths of up to ~100 GPa, which is in good agreement with quantum/atomistic models [14]. Since carbon nanotubes have a low density for a solid of 1.3 to 1.4 g/cm3 [15], its specific strength of up to 48,000 kN·m·kg−1 is the best of known materials, compared to high-carbon steel's 154 kN·m·kg−1.

Under excessive tensile strain, the tubes will undergo plastic deformation, which means the deformation is permanent. This deformation begins at strains of approximately 5% and can increase the maximum strain the tubes undergo before fracture by releasing strain energy.

Although the strength of individual CNT shells is extremely high, weak shear interactions between adjacent shells and tubes leads to significant reductions in the effective strength of multi-walled carbon nanotubes and carbon nanotube bundles down to only a few GPa's [16]. This limitation has been recently addressed by applying high-energy electron irradiation, which crosslinks inner shells and tubes, and effectively increases the strength of these materials to ~60 GPa for multi-walled carbon nanotubes [14] and ~17 GPa for double-walled carbon nanotube bundles [16].

CNTs are not nearly as strong under compression. Because of their hollow structure and high aspect ratio, they tend to undergo buckling when placed under compressive, torsional, or bending stress [17].

Table I: Comparison of mechanical properties [18][19][20][21]

Material	Young's modulus (TPa)	Tensile strength (GPa)	Elongation at break (%)
SWCNT[E]	~1 (from 1 to 5)	13–53	16
Zigzag SWCNT[T]	0.94	94.5	15.6-17.5
Armchair SWCNT[T]	0.94	126.2	23.1
Chiral SWCNT	0.92		
MWCNT[E]	0.2-0.8-0.95	11-63-150	
Stainless Steel[E]	0.186-0.214	0.38-1.55	15-50

2.3.2 Hardness

Standard single-walled carbon nanotubes can withstand a pressure up to 24GPa without deformation. They then undergo a transformation to super hard phase nanotubes. Maximum pressures measured using current experimental techniques are around 55GPa.

However, these new super hard phase nanotubes collapse at an even higher, albeit unknown, pressure.

The bulk modulus of super hard phase nanotubes is 462 to 546 GPa, even higher than that of diamond (420 GPafor single diamond crystal) [22].

2.3.3 Kinetic properties

Multi-walled nanotubes are multiple concentric nanotubes precisely nested within one another. These exhibits a striking telescoping property whereby an inner nanotube core may slide, almost without friction, within its outer nanotube shell, thus creating an atomically perfect linear or rotational bearing. This is one of the first true examples of molecular nanotechnology, the precise positioning of atoms to create useful machines. Already, this property has been utilized to create the world's smallest rotational motor [19]. Future applications such as a gigahertz mechanical oscillator are also envisaged.

2.3.4 Electrical properties

Band structures are computed using tight binding approximation for (6, 0) CNT (zigzag, metallic) (10, 2) CNT (semiconducting) and (10, 10) CNT (armchair, metallic).

Because of the symmetry and unique electronic structure of graphene, the structure of a nanotube strongly affects its electrical properties. For a given (n, m) nanotube, if n = m, the nanotube is metallic; if n − m is a multiple of 3, then the nanotube is semiconducting with a very small band gap, otherwise the nanotube is a moderate semiconductor. Thus all armchair (n = m) nanotubes are metallic, and nanotubes (6, 4), (9,1), etc. are semiconducting [23].

However, this rule has exceptions, because curvature effects in small diameter carbon nanotubes can strongly influence electrical properties. Thus, a (5,0) SWCNT that should be semiconducting in fact is metallic according to the calculations. Likewise, vice versa-- zigzag and chiral SWCNTs with small diameters that should be metallic have finite gap (armchair nanotubes remain metallic) [23]. In theory, metallic nanotubes can carry an electric current density of 4×10^9 A/cm2, which is more than 1,000 times greater than those of metals such as copper [24], where for copper interconnects current densities are limited by electro migration.

Multi-walled carbon nanotubes with interconnected inner shells show superconductivity with a relatively high transition temperature Tc = 12 K. In contrast, the Tc value is an order of

magnitude lower for ropes of single-walled carbon nanotubes or for MWCNTs with usual, non-interconnected shells [25].

2.3.5 Thermal Properties

All nanotubes are expected to be very good thermal conductors along the tube, exhibiting a property known as "ballistic conduction", but good insulators laterally to the tube axis. Measurements show that a SWCNT has a room-temperature thermal conductivity along its axis of about 3500 W·m−1·K−1 [26]; compare this to copper, a metal well known for its good thermal conductivity, which transmits 385 W·m−1·K−1. A SWNT has a room-temperature thermal conductivity across its axis (in the radial direction) of about 1.52 W·m−1·K−1 [27]; which is about as thermally conductive as soil. The temperature stability of carbon nanotubes is estimated to be up to 2800 °C in vacuum and about 750 °C in air [28].

2.3.6 Optical Properties

Whereas mechanical, electrical and electrochemical (super-capacitor) properties of the carbon nanotubes are well established and have immediate applications, the practical use of optical properties is yet unclear. The tunability of properties is potentially useful in optics and photonics. In particular, light-emitting diodes (LEDs) [29][30] and photo-detectors[31] based on a single nanotube have been produced in the lab. Their unique feature is not the efficiency, which is yet relatively low, but the narrow selectivity in the wavelength of emission and detection of light and the possibility of it’s fine tuning through the nanotube structure. In addition, bolometer [32] and optoelectronic memory [33] devices have been realized on ensembles of single-walled carbon nanotubes.

References

[1] Oberlin, A.; M. Endo, and T. Koyama (1976).*"Filamentous growth of carbon through benzene decomposition". J. Cryst. Growth* 32 (3): 335. Bibcode 1976JCrGr..32..335O. doi:10.1016/0022-0248(76)90115-9

[2] I. Iijima, "*Helical microtubules of graphitic carbon,*" *Nature*, vol. 354, pp. 56–58, (1991)

[3] Bethune, D. S.; et al. (17 June 1993)."*Cobalt-catalysed growth of carbon nanotubes with single-atomic-layer walls*".Nature 363 (6430): 605–607.Bibcode 1993Natur.363..605B. doi:10.1038/363605a0.

[4] Iijima, Sumio; ToshinariIchihashi (17 June 1993). "*Single-shell carbon nanotubes of 1-nm diameter*". Nature 363 (6430): 603–605.Bibcode 1993 Natur.363..603I. doi:10.1038/363603a0.

[5] *http://en.wikipedia.org/wiki/Optical_properties_of_carbon_nanotubes#Kataura_plot* (April 9, 2012)

[6] Mintmire, J.W.; Dunlap, B.I.; White, C.T. (1992). "*Are Fullerene Tubules Metallic?*".Physical Review Letters 68 (5): 631–634.Bibcode 1992PhRvL..68..631M. doi:10.1103/PhysRevLett.68.631. PMID 10045950.

[7] Dekker, C. (1999). "*Carbon nanotubes as molecular quantum wires*".Physics Today 52 (5): 22–28.Bibcode 1999PhT....52e..22D. doi:10.1063/1.882658.

[8] Martel, R.; et al. (2001)."*Ambipolar Electrical Transport in Semiconducting Single-Wall Carbon Nanotubes*". Physical Review Letters 87 (25): 256805. Bibcode 2001PhRvL..87y6805M. doi:10.1103/PhysRevLett.87.256805. PMID 11736597.

[9] Flahaut, E.; et al. (2003). "*Gram-Scale CCVD Synthesis of Double-Walled Carbon Nanotubes*". Chemical Communications 12 (12): 1442–1443.doi:10.1039/b301514a.PMID 12841282.

[10] Cumings, J.; Zettl, A. (2000)."*Low-Friction Nanoscale Linear Bearing Realized from Multiwall Carbon Nanotubes*".Science 289 (5479): 602–604. Bibcode2000Sci...289..602C. doi:10.1126/science.289.5479.602. PMID 10915618.

[11] Treacy, M.M.J.; Ebbesen, T.W.; Gibson, J.M. (1996). "*Exceptionally high Young's modulus observed for individual carbon nanotubes*". Nature 381 (6584): 678–680. Bibcode1996Natur.381..678T. doi:10.1038/381678a0.

[12] Zavalniuk, V.; Marchenko, S. (2011)."*Theoretical analysis of telescopic oscillations in multi-walled carbon nanotubes*". Low Temperature Physics 37 (4): 337. arXiv:0903.2461.Bibcode 2011LTP....37..337Z. doi:10.1063/1.3592692.

[13] Yu, M.-F.; et al. (2000). "*Strength and Breaking Mechanism of Multiwalled Carbon Nanotubes Under Tensile Load*". Science 287 (5453): 637–640.Bibcode 2000Sci...287..637Y. doi:10.1126/science.287.5453.637. PMID 10649994.

[14] Peng, B.; et al. (2008)."*Measurements of near-ultimate strength for multiwalled carbon nanotubes and irradiation-induced crosslinking improvements*".Nature Nanotechnology 3 (10): 626–631.doi:10.1038/nnano.2008.211.

[15] Collins, P.G. (2000). "*Nanotubes for Electronics*". Scientific American: 67–69.

[16] Filleter, T.; *et al.* (2011). "*Ultrahigh Strength and Stiffness in Cross-Linked Hierarchical Carbon Nanotube Bundles*". *Advanced Materials* 23 (25): 2855.doi:10.1002/adma.201100547.

[17] Jensen, K.; *et al.* (2007)."*Buckling and kinking force measurements on individual multiwalled carbon nanotubes*". *Physical Review B* 76 (19): 195436. Bibcode2007PhRvB..76s5436J. doi:10.1103/PhysRevB.76.195436.

[18] Belluci, S. (2005). "*Carbon nanotubes: Physics and applications*". Physica Status Solidi C 2 (1): 34–47.Bibcode 2005PSSCR...2...34B.doi:10.1002/pssc.200460105.

[19] Chae, H.G.; Kumar, S. (2006)."*Rigid Rod Polymeric Fibers*". Journal of Applied Polymer Science 100 (1): 791–802. doi:10.1002/app.22680.

[20] Meo, M.; Rossi, M. (2006)."*Prediction of Young's modulus of single wall carbon nanotubes by molecular-mechanics-based finite element modelling*". Composites Science and Technology 66 (11–12): 1597–1605. doi:10.1016/j.compscitech.2005.11.015.

[21] Sinnott, S.B.; Andrews, R. (2001). "*Carbon Nanotubes: Synthesis, Properties, and Applications*". Critical Reviews in Solid State and Materials Sciences 26 (3): 145–249. Bibcode 2001CRSSM..26..145S. doi:10.1080/20014091104189.

[22] Popov, M.; et al. (2002). "*Superhard phase composed of single-wall carbon nanotubes*". Physical Review B 65 (3): 033408. Bibcode 2002PhRvB..65c3408P. doi:10.1103/PhysRevB.65.033408.

[23] Lu, X.; Chen, Z. (2005). "*Curved Pi-Conjugation, Aromaticity, and the Related Chemistry of Small Fullerenes (C60) and Single-Walled Carbon Nanotubes*". Chemical Reviews 105 (10): 3643–3696. doi:10.1021/cr030093d. PMID 16218563.

[24] Hong, Seunghun; Myung, S (2007). "*Nanotube Electronics: A flexible approach to mobility*". Nature Nanotechnology 2 (4): 207–208.Bibcode 2007NatNa...2..207H. doi:10.1038/nnano.2007.89. PMID 18654263.

[25] J. Haruyama et al. (2006). "*Superconductivity in Entirely End-Bonded Multiwalled Carbon Nanotubes*". Physical Review Letters 96 (5): 057001. arXiv:cond-mat/0509466. Bibcode 2006PhRvL..96e7001T. doi:10.1103/PhysRevLett.96.057001. PMID 16486971.

[26] Pop, Eric *et al.*; Mann, David; Wang, Qian; Goodson, Kenneth; Dai, Hongjie (2005-12-22). "*Thermal conductance of an individual single-wall carbon nanotube above room temperature*".*Nano Letters* 6 (1): 96–100. arXiv:cond-mat/0512624. Bibcode2006NanoL...6...96P.doi:10.1021/nl052145f. PMID 16402794.

[27] Sinha, Saion*et al.*; Barjami, Saimir; Iannacchione, Germano; Schwab, Alexander; Muench, George (2005-06-05). "*Off-axis thermal properties of carbon nanotube films*".*Journal of Nanoparticle Research* 7 (6): 651–657.doi:10.1007/s11051-005-8382-9.

[28] Thostenson, Erik; Li, C; Chou, T (2005)."*Nanocomposites in context*".*Composites Science and Technology* 65 (3–4): 491–516. doi:10.1016/j.compscitech.2004.11.003.

[29] J. A. Misewich et al. (2003). "*Electrically Induced Optical Emission from a Carbon Nanotube FET*". Science 300 (5620): 783–786.Bibcode 2003Sci...300..783M. doi:10.1126/science.1081294. PMID 12730598.

[30] J. Chen et al. (2005). "*Bright Infrared Emission from Electrically Induced Excitons in Carbon Nanotubes*".Science 310 (5751): 1171–1174.Bibcode 2005Sci...310.1171C. doi:10.1126/science.1119177. PMID 16293757.

[31] M. Freitag et al. (2003). "*Photoconductivity of Single Carbon Nanotubes*". Nano Letters 3 (8): 1067–1071. Bibcode 2003NanoL...3.1067F.doi:10.1021/nl034313e.

[32] M. E. Itkis et al. (2006). "*Bolometric Infrared Photoresponse of Suspended Single-Walled Carbon Nanotube Films*".Science 312 (5772): 413–416.Bibcode 2006Sci...312..413I. doi:10.1126/science.1125695. PMID 16627739.

[33] A. Star et al. (2004). "*Nanotube Optoelectronic Memory Devices*". Nano Letters 4 (9): 1587–1591. Bibcode 2004NanoL...4.1587S.doi:10.1021/nl049337f.

Chapter 3

Methodology

3.1 Introduction

To investigate the electromagnetic wave characteristics of SWCNT, it is indeed necessary to develop the analytical expression for attenuation and phase shift of signal while propagating through the SWCNT. Starting with Maxwell's equation we may derive the expression for the above two parameters.

3.2 Mathematical Formulations

Maxwell's Equations are a set of 4 complicated equations that describe the world of electromagnetic. These equations describe how electric and magnetic fields propagate, interact, and how they are influenced by objects.

The four Maxwell equations can be expressed as

$$\nabla \times \vec{H} = \vec{J} + \frac{\partial \vec{D}}{\partial t} \tag{3.1}$$

$$\nabla \times \vec{E} = -\mu \frac{\partial \vec{H}}{\partial t} \tag{3.2}$$

$$\nabla \cdot \vec{H} = 0 \tag{3.3}$$

$$\nabla \cdot \vec{E} = \rho \tag{3.4}$$

where H is the magnetic field intensity, J is the current density, D is the electric displacement field, and E is the electric field.

Also, Ohm's law can be expressed as

$$\vec{J} = \sigma \vec{E}. \tag{3.5}$$

From (3.2), one can write the following:

$$\nabla \times \nabla \times \vec{E} = -\mu \frac{\partial}{\partial t}(\nabla \times \vec{H}). \tag{3.6}$$

Now, recall the vector identity

$$\nabla \times \nabla \times \vec{E} = \nabla(\nabla \cdot \vec{E}) - \nabla^2 \vec{E}. \tag{3.7}$$

Note that there is no source charge in the system ($\rho = 0$), so that (3.4) can be written as $\nabla \cdot E = 0$. Hence, substituting (3.7) in (3.6), one arrives at

$$\nabla^2 \vec{E} = \mu \frac{\partial}{\partial t}(\nabla \times \vec{H}). \tag{3.8}$$

Substituting (3.1) and (3.5) into (3.8) leads to

$$\nabla^2 \vec{E} = \mu \frac{\partial}{\partial t}(\sigma \vec{E} + \frac{\partial \vec{D}}{\partial t}). \tag{3.9}$$

For a good conductor, the displacement current is negligible, compared with the conduction current, so that the second item on the right-hand side of (3.9) is negligible. Thus, (3.9) can be further written as

$$\nabla^2 \vec{E} = \mu\sigma \frac{\partial}{\partial t} \vec{E}. \tag{3.10}$$

For a time-varying field, the electric field can be written as

$\vec{E} = \vec{E}_0 e^{j\omega t}$, so that

$$\frac{\partial}{\partial t} \vec{E} = \frac{\partial}{\partial t} \vec{E}_0 e^{j\omega t} = j\omega \vec{E}_0 e^{j\omega t} = j\omega \vec{E}. \tag{3.11}$$

Substituting (3.11) in (3.10), one arrives at

$$\nabla^2 \vec{E} = j\omega\mu\sigma\vec{E}. \tag{3.12}$$

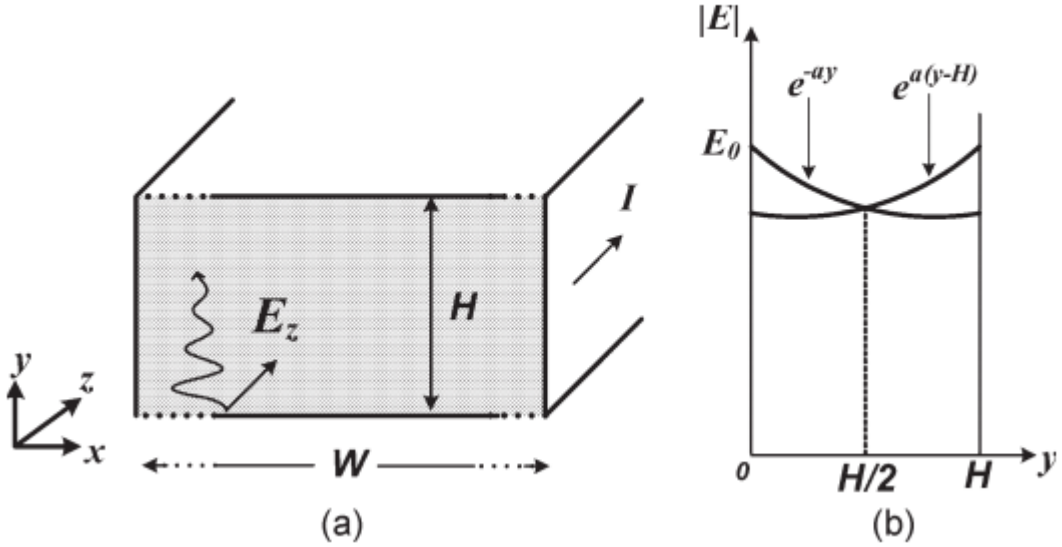

Figure.3.1. (a) Conductor with height *H* and semi-infinite width (*W*» *H*) and length. The EM wave propagates in the *y*-direction (with the current and *E*-field in the *z* direction). (b) Schematic illustration of the decay of electric field inside the conductor along the height (*y* direction).

For a good conductor, where displacement current is negligible compared to the conduction current (e.g., $\omega\varepsilon\ \sigma$), one can derive the following relation from the Maxwell's equations:

$$\nabla^2 \vec{E} = j\omega\mu\sigma\vec{E} \tag{3.13}$$

where μ and σ are the permeability and conductivity of the material, respectively. Considering a semi-infinite material [as shown in Figure. 2.1(a)] with height *H*, width *W* (*W* >> *H*), and with current (or *E*-field) in the *z* direction, the electrical field propagation in the direction that is perpendicular to the $x - z$ surface (*y* direction) will follow (3.13), whose 1-D form is

$$\frac{d^2 E_z}{dy^2} = j\omega\mu\sigma E_z = \Gamma^2 E_z \tag{3.14}$$

Where

$$\Gamma = \sqrt{j\omega\mu\sigma} = \alpha + j\beta \tag{3.15}$$

And E_z can be solved as

$$E_z = E_0 e^{-\Gamma y} = E_0 e^{-\alpha y - j\beta y} \tag{3.16}$$

The first exponential component $e^{-\alpha y}$ represents the exponential decay of electrical field in y direction inside the conductor, as shown in Figure.2.1 (b). The second exponential component $e^{-j\beta y}$ represents the E-field propagation along y direction. Substituting $\sigma(\omega) = \sigma 0/(1 + j\omega\tau)$ into (3.16), α and β are obtained as

$$\alpha = \sqrt{\frac{\omega\mu\sigma_0}{2}} \cdot \sqrt{\frac{1}{(\omega\tau)^2 + 1}\left[\sqrt{(\omega\tau)^2 + 1} + \omega\tau\right]} \tag{3.17}$$

$$\beta = \sqrt{\frac{\omega\mu\sigma_0}{2}} \cdot \sqrt{\frac{1}{(\omega\tau)^2 + 1}\left[\sqrt{(\omega\tau)^2 + 1} - \omega\tau\right]} \tag{3.18}$$

The skin depth δ is defined as $1/\alpha$, which is

$$\delta = \sqrt{\frac{2}{\omega\mu\sigma_0}} \cdot \sqrt{[(\omega\tau)^2 + 1] \cdot \left[\sqrt{(\omega\tau)^2 + 1} - \omega\tau\right]} \tag{3.19}$$

For conventional metals (τ is very small or $\omega\tau \ll 1$),(3.19) reduces to the classical skin depth

$$\delta_c = \sqrt{2/\omega\mu\sigma_0} \tag{3.20}$$

For CNTs, the momentum relaxation time can be obtained by

$$\tau = \frac{\tau_B}{2} = \frac{\lambda}{2\nu_F} \approx \frac{500D}{\nu_F} \tag{3.21}$$

References

[1] David J Griffiths (1999). *Introduction to electrodynamics* (Third ed.). Prentice Hall. pp. 559–562. ISBN 0-13-805326-X.
[2] Hong Li, and K. Banerjee, "High-frequency analysis of carbon nanotube interconnects and implications for on-chip inductor design," *IEEE Trans. Electron Devices*, vol. 56, No. 10, 2009
[3] D. M Pozar, *Microwave Engineering*; Wiley: New York, 1998. pp. 63-64
[4] "IEEEGHN: Maxwell's Equations". Ieeeghn.org. Retrieved 2008-10-19.

Chapter 4

Results and Discussion

4.1 Results and discussion

To investigate the attenuation and phase shift characteristics we developed the MATLAB code to predict the evolution of attenuation versus frequency and diameter of SWCNT. The MATLAB code is shown in Appendix.

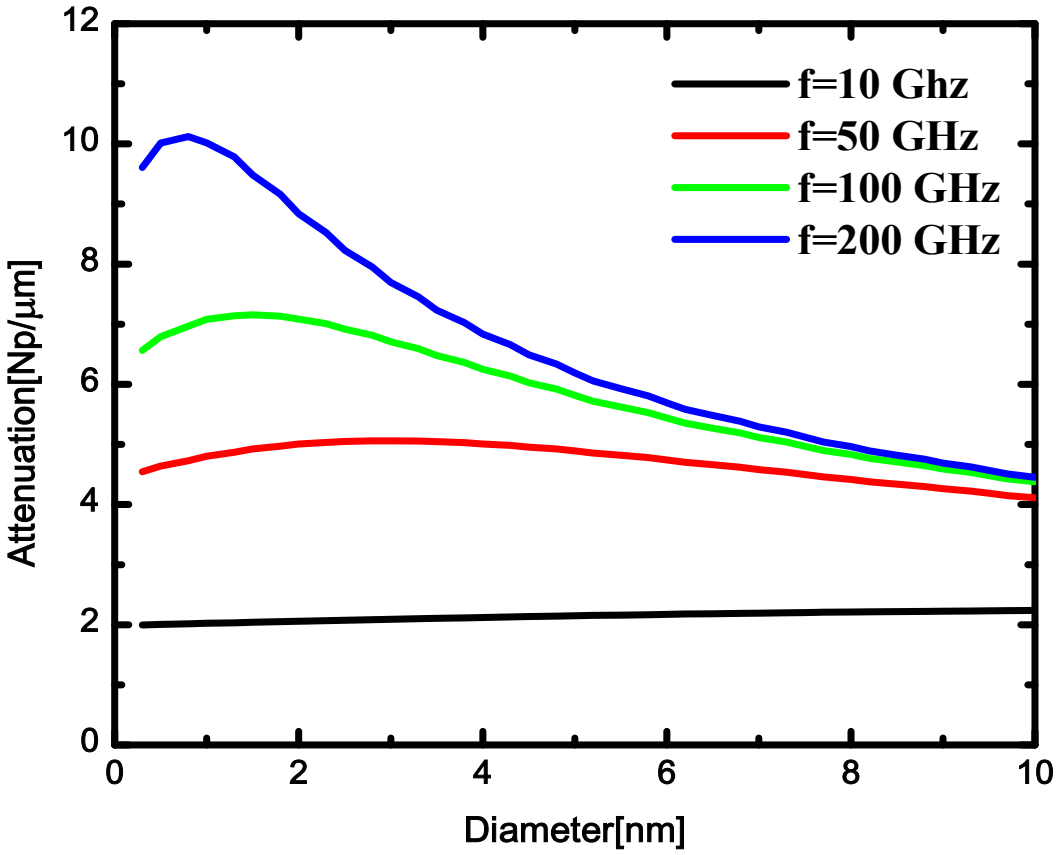

Fig 4.1 Change of attenuation with diameter at different frequencies

For different frequencies we increased the diameter of SWCNT and analyzed the change in attenuation. From Fig 4.1 we can see that higher frequency gives higher attenuation. It is found that with the increase of diameter of SWCNT the attenuation reduces gradually.

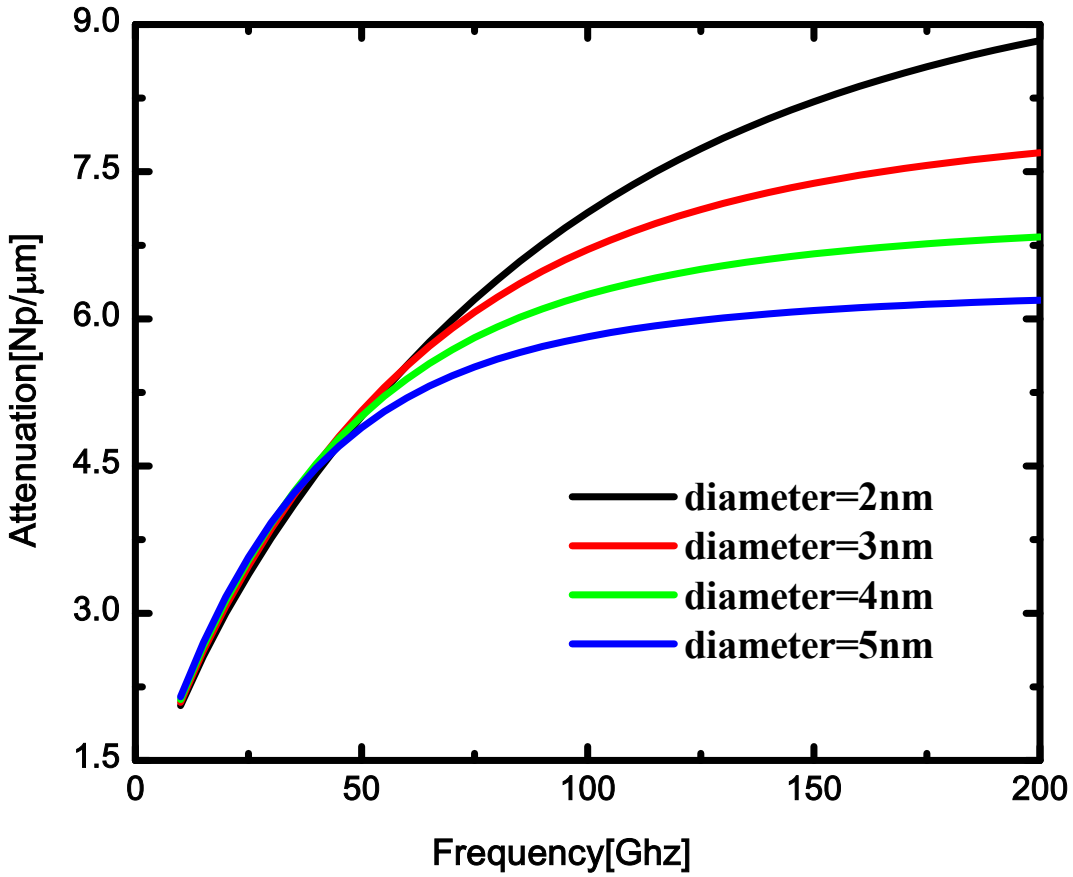

Fig 4.2 Change of attenuation with frequency at different diameter

For different diameters we increased the frequency of SWCNT and analyzed the change in attenuation. From Fig 4.2 we can see that higher frequency gives higher attenuation. And by increasing the diameter of SWCNT the attenuation reduces gradually.

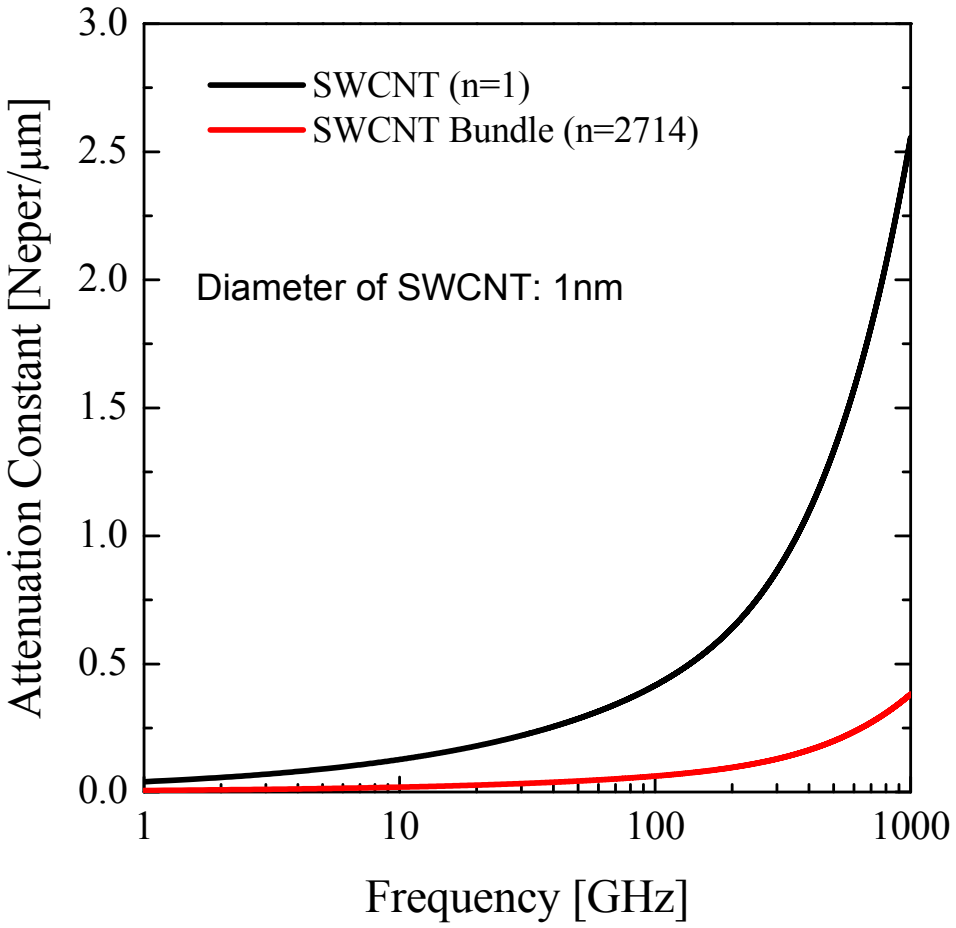

Figure.4.3 Frequency dependence of attenuation constant for single SWCNT and bundled SWCNT

Figure 4.3 shows the evolution of attenuation constant with frequency. Attenuation constant increases with the increase of frequency due to the reduction of skin depth at higher frequency and attenuation constant is inversely proportional to skin depth. It is also found that the attenuation is much lower in a bundle of SWCNT than that of in a single SWCNT.

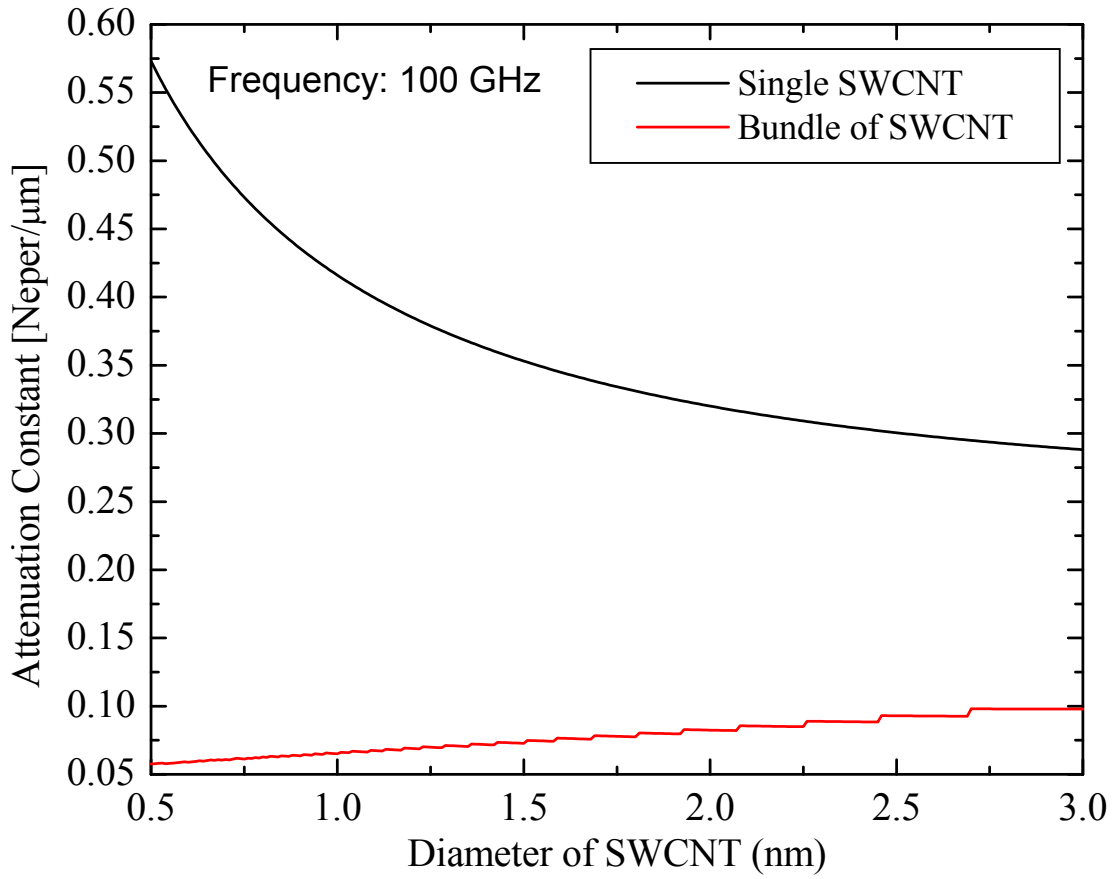

Figure 4.4 Effects of SWCNT's diameter on the attenuation constant at 100 GHz.

Figure 4.4 shows the effects of diameter of SWCNT on the attenuations constant of single and bundled SWCNTs at 100 GHz. It is found that in single SWCNT attenuation constant decreases with larger diameter, because larger diameter CNTs offer smaller resistance. On the other hand, the attenuation of bundled SWCNT slightly increases with diameter.

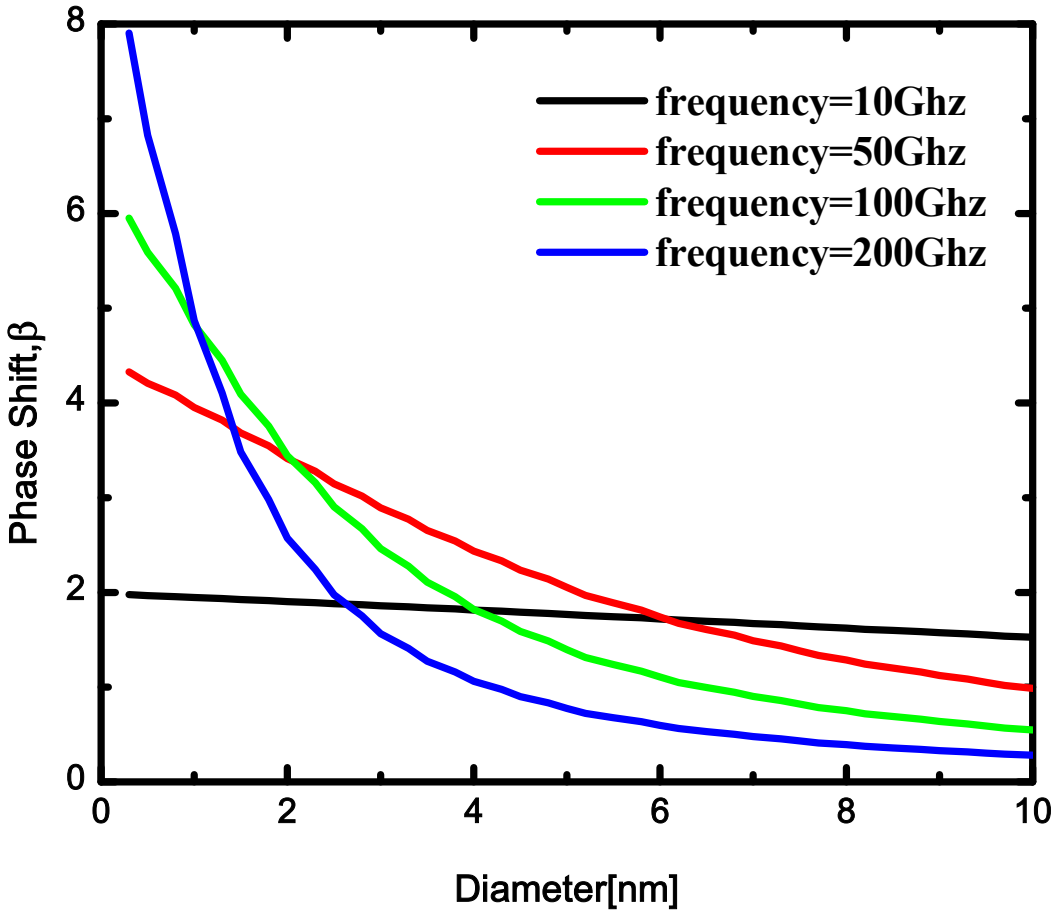

Fig.4.5 Change of phase shift with diameter at different frequencies

For different diameter we increased the frequency of SWCNT and analyzed the change in phase shift. From Fig 4.5 we can see that larger diameter gives least phase shift for increasing frequency. And by increasing the frequency of SWCNT the phase shift reduces gradually and gives the lowest for larger diameter.

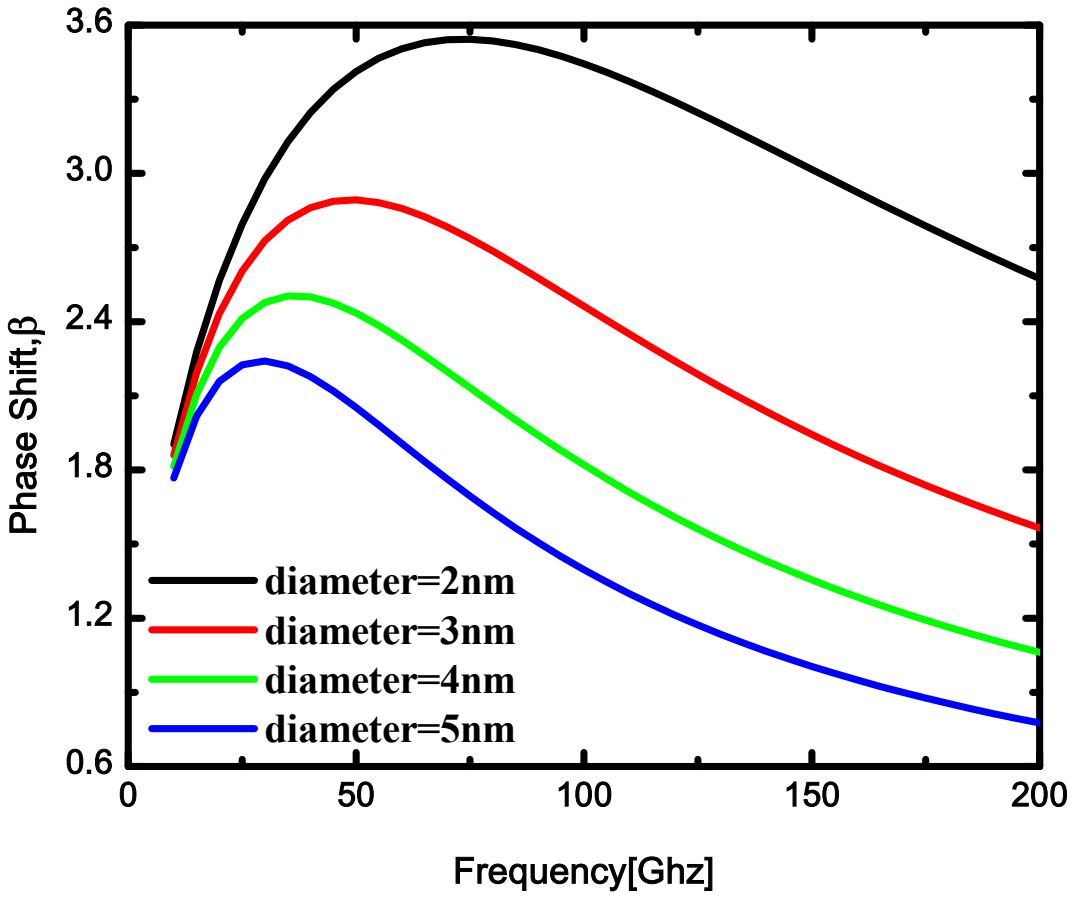

Fig.4.6 Change of phase shift with frequency at different diameter of SWCNT.

For different diameter we increased the frequency of SWCNT and analyzed the change in phase shift. From Figure 4.6 we can see that larger diameter gives least phase shift for increasing frequency. And by increasing the frequency of SWCNT the phase shift reduces gradually and gives the lowest for larger diameter.

Chapter 5

Conclusions

In this thesis the expressions for phase shift, and attenuation constant have been derived starting with Maxwell's electromagnetic field equations for SWCNT. We have discussed the electrical, mechanical and optical properties of single SWCNT. It is found that attenuation is a strong functions of frequency and diameter of SWCNT. It is found that in single SWCNT attenuation constant decreases with larger diameter, because larger diameter CNTs offer smaller resistance. On the other hand, the attenuation of bundled SWCNT slightly increases with diameter. It may be recommended that to have smaller attenuation, we should use larger diameter SWCNTs.

Appendix

A.1. MATLAB code for finding attenuation vs diameter:

```
U=4*pi*10^-7

W2=2*pi*10*10^9;

W3=2*pi*50*10^9;

W4=2*pi*100*10^9;

W5=2*pi*200*10^9;

D=[.25e-9:.25e-9:10e-9]

T=(1000.*D)./(2*8*10^5);

S2=sqrt(2./(9.99e7*W2*U)).*sqrt(((W2.*T).^2)+1).*sqrt(sqrt(((W2.*T).^2)+1)-W2.*T)

S3=sqrt(2./(9.99e7*W3*U)).*sqrt(((W3.*T).^2)+1).*sqrt(sqrt(((W3.*T).^2)+1)-W3.*T)

S4=sqrt(2./(9.99e7*W4*U)).*sqrt(((W4.*T).^2)+1).*sqrt(sqrt(((W4.*T).^2)+1)-W4.*T)

S5=sqrt(2./(9.99e7*W5*U)).*sqrt(((W5.*T).^2)+1).*sqrt(sqrt(((W5.*T).^2)+1)-W5.*T)

A4=1./S4

A3=1./S3

A2=1./S2

A5=1./S5

plot(D,A2,'r');hold on

plot(D,A3,'g');hold on
```

```
plot(D,A4,'y');hold on

plot(D,A5,'b');

Xlabel('Diameter')

Ylabel('Attenuation');

legend('f=10Ghz','f=50Ghz','f=100Ghz','f=200Ghz');

fid = fopen('atten_vs_diameter.doc','w');

fprintf(fid,'%10.10f\r\t\n',D, A2, A3, A4, A5);

fclose(fid);
```

A.2 MATLAB code for finding attenuation vs frequency:

```
U=4*pi*10^-7

F=[10e9:5e9:200e9]

W1=2*pi*F;

W2=2*pi*F;

W3=2*pi*F;

W4=2*pi*F;

D1= 2e-9;

D2= 3e-9;

D3= 4e-9;

D4= 5e-9;
```

```
T1=(1000.*D1)./(2*8*10^5);

T2=(1000.*D2)./(2*8*10^5);

T3=(1000.*D3)./(2*8*10^5);

T4=(1000.*D4)./(2*8*10^5);

S1=sqrt(2./(9.99e7*W1*U)).*sqrt(((W1.*T1).^2)+1).*sqrt(sqrt(((W1.*T1).^2)+1)-W1.*T1)

S2=sqrt(2./(9.99e7*W2*U)).*sqrt(((W2.*T2).^2)+1).*sqrt(sqrt(((W2.*T2).^2)+1)-W2.*T2)

S3=sqrt(2./(9.99e7*W3*U)).*sqrt(((W3.*T3).^2)+1).*sqrt(sqrt(((W3.*T3).^2)+1)-W3.*T3)

S4=sqrt(2./(9.99e7*W4*U)).*sqrt(((W4.*T4).^2)+1).*sqrt(sqrt(((W4.*T4).^2)+1)-W4.*T4)

A3=1./S3

A2=1./S2

A1=1./S1

A4=1./S4

plot(F,A1,'r');hold on

plot(F,A2,'g');hold on

plot(F,A3,'y');hold on

plot(F,A4,'b');

Xlabel('Frequency')

Ylabel('Attenuation');

legend('D=2nm','D=3nm','D=4nm','D=5nm');

fid = fopen('atten_vs_frequency.doc','w');

fprintf(fid,'%10.10f\r\t\n',F, A1, A2, A3, A4);
```

```
fclose(fid);
```

A.3 Matlab Codes for determining Attenuation vs Diameter:

```
U=4*pi*10^-7

W1=2*pi*10*10^9;

W2=2*pi*50*10^9;

W3=2*pi*100*10^9;

W4=2*pi*200*10^9;

D=[.25e-9:.25e-9:10e-9]

T=(1000.*D)./(2*8*10^5);

B1=sqrt((9.99e7*W1*U)/2).*sqrt(1./(((W1.*T).^2)+1)).*sqrt(sqrt(((W1.*T).^2)+1)-W1.*T)

B2=sqrt((9.99e7*W2*U)/2).*sqrt(1./(((W2.*T).^2)+1)).*sqrt(sqrt(((W2.*T).^2)+1)-W2.*T)

B3=sqrt((9.99e7*W3*U)/2).*sqrt(1./(((W3.*T).^2)+1)).*sqrt(sqrt(((W3.*T).^2)+1)-W3.*T)

B4=sqrt((9.99e7*W4*U)/2).*sqrt(1./(((W4.*T).^2)+1)).*sqrt(sqrt(((W4.*T).^2)+1)-W4.*T)

plot(D,B1,'r');hold on

plot(D,B2,'g');hold on

plot(D,B3,'y');hold on

plot(D,B4,'b');

Xlabel('Diameter')

Ylabel('Beta');

legend('f=10Ghz','f=50Ghz','f=100Ghz','f=200Ghz');
```

```
fid = fopen('beta.doc','w');

fprintf(fid,'%10.10f\r\t\n',D, B1, B2, B3, B4);

fclose(fid);
```

A.4 Matlab Code for determining Attenuation vs Frequency:

```
U=4*pi*10^-7

F=[10e9:5e9:200e9]

W1=2*pi*F;

W2=2*pi*F;

W3=2*pi*F;

W4=2*pi*F;

D1= 2e-9;

D2= 3e-9;

D3= 4e-9;

D4= 5e-9;

T1=(1000.*D1)./(2*8*10^5);

T2=(1000.*D2)./(2*8*10^5);

T3=(1000.*D3)./(2*8*10^5);

T4=(1000.*D4)./(2*8*10^5);

B1=sqrt((9.99e7*W1*U)/2).*sqrt(1./(((W1.*T1).^2)+1)).*sqrt(sqrt(((W1.*T1).^2)+1)-W1.*T1)

B2=sqrt((9.99e7*W2*U)/2).*sqrt(1./(((W2.*T2).^2)+1)).*sqrt(sqrt(((W2.*T2).^2)+1)-W2.*T2)

B3=sqrt((9.99e7*W3*U)/2).*sqrt(1./(((W3.*T3).^2)+1)).*sqrt(sqrt(((W3.*T3).^2)+1)-W3.*T3)
```

```
B4=sqrt((9.99e7*W4*U)/2).*sqrt(1./(((W4.*T4).^2)+1)).*sqrt(sqrt(((W4.*T4).^2)+1)-W4.*T4)

plot(F,B1,'r');hold on

plot(F,B2,'g');hold on

plot(F,B3,'y');hold on

plot(F,B4,'b');

Xlabel('Frequency')

Ylabel('Beta');

legend('D=2nm','D=3nm','D=4nm','D=5nm');

fid = fopen('beta_vs_freq.doc','w');

fprintf(fid,'%10.10f\r\t\n',F, B1, B2, B3, B4);

fclose(fid);
```